Presented to ASME Forum on Active Noise Control-Work in Progress
IMECE, Dallas
November 1997

A SMART HELMHOLTZ RESONATOR

Charles B. Birdsong
Department of Mechanical Engineering
Michigan State University
East Lansing, MI 48824-1229

Clark J. Radcliffe
Department of Mechanical Engineering
Michigan State University
East Lansing, MI 48824-1229

ABSTRACT

Helmholtz resonators are commonly used for tuning of acoustic systems such as industrial processes, vehicle exhaust, engine intake manifold systems and more. Past efforts resulted in limited tuning capability and significant mechanical complexity. The work presented here considers a system that modifies the acoustic response of a system continuously, on-line, allowing optimum performance over a range of operating conditions in contrast to discrete points. The system consists of a static Helmholtz resonator designed to enforce a nominal resonance and an active control of an audio speaker that provides a variable acoustic impedance. The combination of the nominal impedance of the resonator and the differential impedance of the control speaker results in a active controlled, variable frequency Helmholtz resonator, named for simplicity the "Smart Helmholtz Resonator." The system is modeled using bond graph methods and state space formulation is used to analyze the frequency response.

INTRODUCTION

The Helmholtz resonator (HR) is an ideal, simple acoustic device that has applications in acoustic systems. In acoustic system design, a HR is often used to modify the acoustic response. For example, internal combustion engine intake manifold systems are designed so that the acoustic response enhances the engine performance, increases fuel economy and reduces emissions (Kong, Woods, 1992). When design considerations such as space and material limitations cause the acoustic response to degrade engine performance and/or create excessive noise, the solution is often to add a designed HR to the system, thus improving the response.

Tuning of engine intake manifold systems is commonly used in the automobile industry. Engine performance can be greatly improved by designing the dimensions of the intake manifold system to improve the engine "breathing" (Jameson, Hodgins, 1990). More recently, efforts have been made to change the acoustic response of the intake manifold system on-line. The GM 4.3L V6 engine uses a butterfly valve to change the manifold acoustic response between two configurations at a given engine speed (Grahm et al., 1992). The result is an engine that is tuned at two speeds, instead of one, and thus has greater performance and higher fuel economy. Another model, the engine in the Mazda Wankel engine powered car changes the length of the acoustic space in the intake manifold continuously as the engine speed changes using a unwinding coiled acoustic duct (Garret, 1992). The result is an engine that can be tuned at a range of frequencies and thus improved performance over a range of engine speeds. However the complex mechanism used to control and link the coil duct to the engine adds significant complexity to the manifold design.

This paper considers the solution of using active control to modify the acoustic response of a HR in real time. A successful working model of the Smart HR could be used in engine intake manifold systems to continuously tune the engine over a range of operating speeds and thus improve engine performance over a wide range of operating speeds. This system would function as a self-contained device with few moving parts and integrate smoothly with the manifold system, thus eliminating the complexity of changing the physical dimensions of the acoustic system during operation.

MODEL DEVELOPMENT

The model of the Smart Helmholtz Resonator (SHR) consists of an ideal HR, with a complex impedance boundary condition. A controller is used to implement the boundary condition and bond graph modeling and frequency response is used to analyze the resulting system.

An ideal HR is an acoustic resonant system whose volumetric flow u_a, to input pressure, P_{in} relationship can be represented by a second order transfer function. The HR consists of a rigid-wall cavity and at least one short and narrow orifice thorough which the fluid filling it communicates with the external medium (Temkin, 1936) as shown in Figure 1.

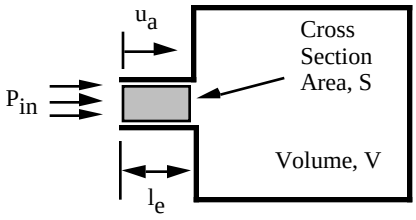

Figure 1: Ideal Helmholtz Resonator

The complex acoustic impedance of the HR, z relates the pressure P_{in} in the cavity to the acoustic velocity u_a flowing into the cavity as

$$P_{in} = zu_a \tag{1}$$

The complex impedance for a HR is given as (Temkin, 1936)

$$z = R' + i\rho_o \left(\frac{\omega c_o^2 S}{V\omega} - \omega l_e \right) \tag{2}$$

where R' is the resistance due to radiation losses, ρ_o is the density of the medium, c_o is the speed of sound in the medium, S is the cavity orifice cross sectional area, and V is the cavity volume. When dissipation is very small resonance occurs at a frequency

$$\omega = c_o \sqrt{1/C_a I_a} \tag{3}$$

where C_a and I_a are the effective compliance and inertia respectively and are given by

$$C_a = \frac{V}{\rho_o c_o^2 S} \tag{4}$$

$$I_a = \rho_o l_e \tag{5}$$

and l_e is the length of the cavity orifice opening.

The acoustic loss associated with the R' term in (2) will be small for the system in this study and is therefore neglected in the following analysis. Although this term could be carried throughout the derivation, it increases the order of the transfer functions and adds considerable complexity to the results, obscuring the overall resonant nature of the system, while adding little information. With this assumption, a transfer function representation of the system is given by

$$\frac{u_a}{P_{in}} = \frac{1}{I_a} \left[\frac{s}{s^2 + \frac{1}{C_a I_a}} \right] \tag{6}$$

The ideal HR model can be modified by adding a boundary condition to modify the system dynamics (Radcliffe, Gogate, 1994). Figure 2 shows a HR with a massless piston connected to a boundary condition indicated by an element labeled 'G(s)' where G(s) is a transfer function relating the piston displacement x_m to the force acting on the piston.

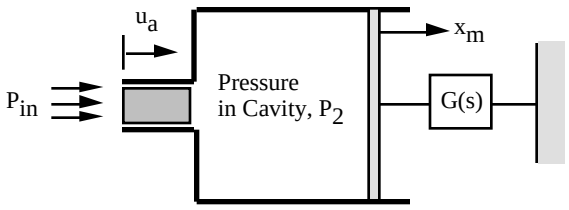

Figure 2. HR with Complex Impedance Boundary Condition

The impedance will be implemented by an electro-mechanical sensor-controller-actuator system resulting in a multidomain system. Bond graph modeling is a powerful method for forming multidomain system models and will be used here (Karnopp et. at. 1990). This method will be further justified when the model complexity is increased. Figure 3 shows the bond graph model with the complex boundary condition. The input pressure is represented by a source of effort Se, the acoustic inertia and compliance of the HR are represented by the I and C elements respectively, and the complex impedance is represented by the G(s) element. The 1 junction represents the fluid velocity in the neck of the HR and the 0 junction represents the pressure in the cavity. The causality of each element in the system is indicated by the causal stroke. All acoustic elements have integral causality and the causal stroke on the complex impedance indicates that an effort (pressure) is input to the G(s) element which returns a flow (velocity). This action can be implemented with a microphone to sense pressure and an audio speaker to return a velocity flow rate.

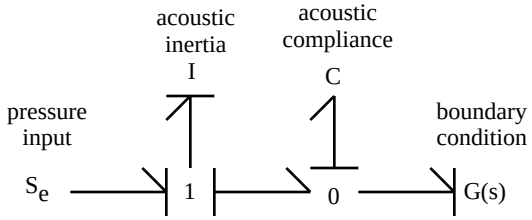

Figure 3. HR with Complex Impedance Bond Graph Model

The causal stroke on the bond graph model indicates that the correct causality for G(s) is given by

$$u_m = G(s) P_{in} \tag{7}$$

where P_{in} is the input and the velocity u_m is the output.

State equations can be written for the bond graph model taking u_a and x_m as the states giving

$$\begin{bmatrix} \dot{u}_a \\ \dot{x}_m \end{bmatrix} = \begin{bmatrix} 0 & \frac{-1}{C_a I_a} \\ 1 & \frac{-G(s)}{C_a} \end{bmatrix} \begin{bmatrix} u_a \\ x_m \end{bmatrix} + \begin{bmatrix} \frac{1}{I_a} \\ 0 \end{bmatrix} P_{in} \tag{8}$$

The transfer function that relates the input pressure to the acoustic velocity can then be found as

$$\frac{u_a}{P_{in}} = \frac{1}{I_a} \left[\frac{s + \frac{G(s)}{C_a}}{s^2 + \frac{G(s)}{C_a} s + \frac{1}{C_a I_a}} \right] \tag{9}$$

The dynamic response of the system can be modified by designing the transfer function G(s). Consider replacing the impedance with a Proportional-Integral-Derivative Control transfer function defined by

$$G(s) = K_P + \frac{K_I}{s} + K_D s \tag{10}$$

where K_P, K_I and K_D are the proportional, integral and derivative gains respectively.

The closed loop transfer function can be computed by replacing G(s) in (9) with (10) and simplifying which gives

$$\frac{u_a}{P_{in}} = \frac{1}{I_a}\left[\frac{(K_D + C_a)s^2 + K_P s + K_I}{(K_D + C_a)s^3 + K_P s^2 + \left(K_I + \frac{1}{I_a}\right)s}\right] \qquad (11)$$

Some intuitive understanding of the effect of K_P, K_I and K_D on the response of the system can be obtained by studying (11). For example it is clear that K_D appears only as a term that is added to C_a. This suggests that K_D effects the roots of the transfer function in the same way as C_a. Also, K_I appears in the denominator as a term that is added to the inverse of the inertia suggesting that it effects the roots of the transfer function in a similar manner as I_a.

A more clear view is given by considering each term separately. Taking K_D while setting K_P and K_I equal to zero in (11) gives

$$\frac{u_a}{P_{in}} = \frac{1}{I_a}\left[\frac{s}{s^2 + \frac{1}{I_a(C_a + K_D)}}\right] \qquad (12)$$

which shows that K_D acts as a compliance in series with the acoustic compliance.

Taking K_P while setting K_I and K_D equal to zero in (11) gives

$$\frac{u_a}{P_{in}} = \frac{1}{I_a}\left[\frac{C_a s + K_P}{C_a s^2 + K_P s + \frac{1}{I_a}}\right] \qquad (13)$$

which shows that a term has been added that acts as a damping term that is proportional to K_P.

Taking K_I and setting K_P and K_D equal to zero in (11) gives

$$\frac{u_a}{p} = \frac{1}{I_a}\left[\frac{C_a s^2 + K_I}{C_a s^2 + K_I + \frac{1}{I_a}s}\right] \qquad (14)$$

which shows that K_I combines with the inertia term. These results can be illustrated by plotting the frequency response of the system for each type of controller as shown in Figures 4, 5, and 6. Values used for the model parameters were $V = 0.00742\ m^3$, $\rho_o = 1.18\ Kg/m^3$, $c_o = 343\ m/s$, $S = 0.000113\ m^2$, and $l_e = 0.055\ m$.

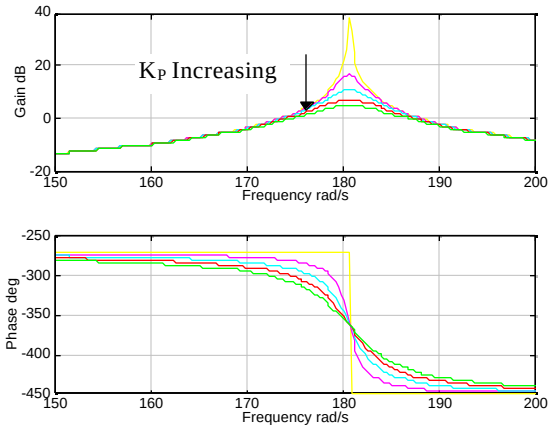

Figure 4: Bode Diagram for Proportional Controller with K_P Ranging from 0 to 0.04

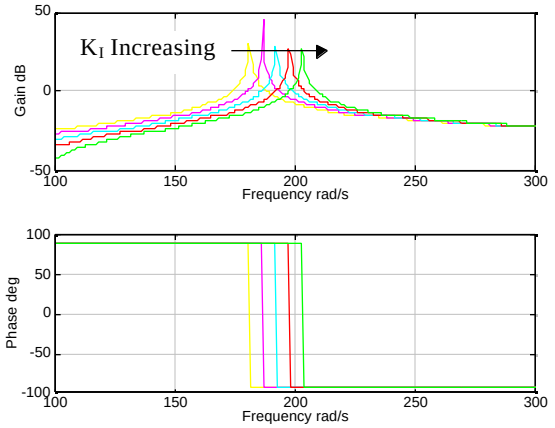

Figure 5: Bode Diagram for Integral Controller with K_I Ranging from 0 to 4

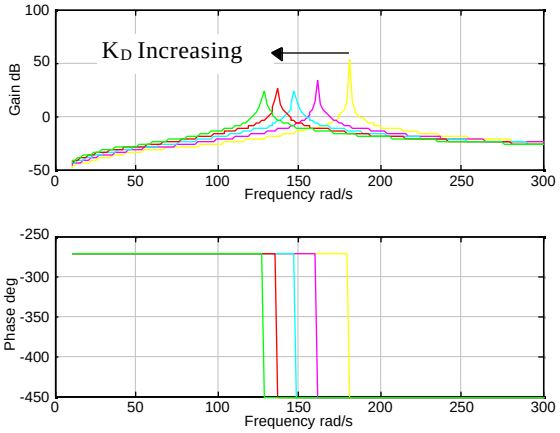

Figure 6: Bode Diagram for Derivative Controller with K_D Ranging from 0 to 5E-4.

These figures illustrate the ability of the SHR to change the dynamic response of the system. Each gain K_P, K_I, K_D gives an input to change the apparent inertia, damping and compliance of the HR. In each case the resonance is preserved but the resonant frequency or damping is altered. The advantage of this effect is that the response of the HR is modified without changing the physical dimensions, i.e. cavity volume, neck length or cross section area. The change in response is caused only by the interaction of the boundary condition with the HR.

This design also has the benefit that when the boundary condition is removed, i.e. the controller is turned off, the system reverts to the nominal resonance defined by the physical dimensions of the HR. Since these dimensions can designed to meet nominal performance requirements, turning off the controller will only remove the variable tuning leaving the nominal tuning in tact.

Another important design consideration of this system is that the sensitive moving parts, microphone and actuator are not directly in the path of the fluid flow. Instead, they are located inside of the HR. This provides the advantage that debris carried by the fluid in the system will not come in direct contact with the microphone and actuator. Failure due to fouling from debris and harsh environmental conditions has limited previous implementations of active automotive muffler systems.

MODELING THE COMPLEX BOUNDARY CONDITION

The model can be made more realistic by replacing the ideal boundary condition G(s) with a model of a physical system, namely a microphone, controller, and speaker that produces the desired boundary condition response. The bond graph model given in Figure 7 is augmented by adding a microphone to sense the pressure in the HR, and a controller and actuator to produce the desired volumetric flow rate at the boundary. The actuator model uses internal compensation to eliminate the speaker internal resonance and the dynamics due to the pressure interactions with the HR (Birdsong 1996), (Radcliffe, Gogate, 1996), (Radcliffe, Gogate, 1992).

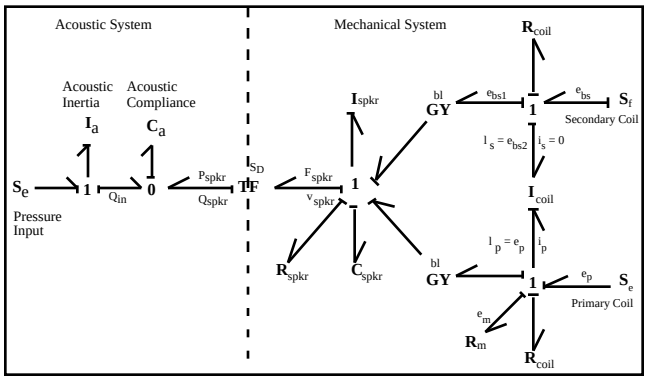

Figure 7: Bond Graph Model of SIR with Microphone, Controller and Actuator

The state equations of the HR and actuator in open-loop can be assembled from bond graph model and are given by

$$\frac{d}{dt}\begin{bmatrix} v_a \\ x_a \\ v_s \\ x_s \\ \lambda \\ i_p \end{bmatrix} = \begin{bmatrix} 0 & \frac{-1}{C_a I_a} & 0 & 0 & 0 & 0 \\ 1 & 0 & S_d & 0 & 0 & 0 \\ 0 & \frac{-S_d}{I_s C_a} & \frac{-R_s}{I_s} & \frac{-1}{C_s I_s} & \frac{bl}{I_c I_s} & 0 \\ 0 & 0 & 1 & 0 & 0 & 0 \\ 0 & 0 & -bl & 0 & \frac{-R_m - R_c}{I_c} & 0 \\ 0 & 0 & 0 & 0 & 0 & 0 \end{bmatrix} \begin{bmatrix} v_a \\ x_a \\ v_s \\ x_s \\ \lambda \\ i_p \end{bmatrix} + \begin{bmatrix} 0 & 0 & \frac{1}{I_a} \\ 0 & 0 & 0 \\ \frac{bl}{I_s}\left(1 - \frac{M_c}{I_c}\right) & 0 & 0 \\ 0 & 0 & 0 \\ M_c\frac{R_c + R_m}{I_c} & 1 & 0 \\ 0 & 0 & 0 \end{bmatrix} \begin{bmatrix} i_{bl} \\ e_p \\ P_{in} \end{bmatrix} \tag{15}$$

The output equation is given by

$$\begin{bmatrix} v_a \\ e_{bs} \\ i_p \\ P_{spkr} \end{bmatrix} = \begin{bmatrix} 1 & 0 & 0 & 0 & 0 & 0 \\ 0 & 0 & bl\left(1 - \frac{M_c}{I_c}\right) & 0 & \frac{-M_c}{I_c^2}(R_c + R_m) & 0 \\ 0 & 0 & 0 & 0 & \frac{1}{I_c} & 0 \\ 0 & \frac{1}{C_a} & 0 & 0 & 0 & 0 \end{bmatrix} \begin{bmatrix} v_a \\ x_a \\ v_s \\ x_s \\ \lambda \\ i_p \end{bmatrix} + \begin{bmatrix} 0 & 0 & 0 \\ 0 & \frac{M_c}{I_c} & 0 \\ 0 & 0 & 0 \\ 0 & 0 & 0 \end{bmatrix} \begin{bmatrix} i_{bl} \\ e_p \\ P_{in} \end{bmatrix} \tag{16}$$

where the states are the acoustic velocity and displacement at the HR neck V_A, and x_a, the speaker face velocity and displacement v_s, and x_s, and the electromagnetic flux in the speaker coil λ. The inputs are the primary coil current i_p, the primary coil voltage e_p and the input pressure to the HR neck P_{in}, and the outputs are the acoustic velocity v_a, the voltage in the secondary coil e_{bs}, the current in the primary coil i_p and the pressure at the speaker face P_{spkr}. The new parameters in (15) and (16) relate to the compensated acoustic actuator model and are the speaker face area, S_d, the speaker inertia I_s, speaker compliance C_s, speaker friction R_s, speaker coil resistance R_c, speaker coil inductance I_c, speaker coil mutual inductance M_c, speaker electromechanical coupling factor bl, and the primary coil current sensing resistance R_m.

The closed loop response of the system can be computed by applying the speaker compensation and feeding the output P_{spkr} to the controller then to the input of the actuator as illustrated in Figure 8. The blocks H_p, H_{bs}, and K_1 implement the speaker compensation. This model represents the SHR in the final form.

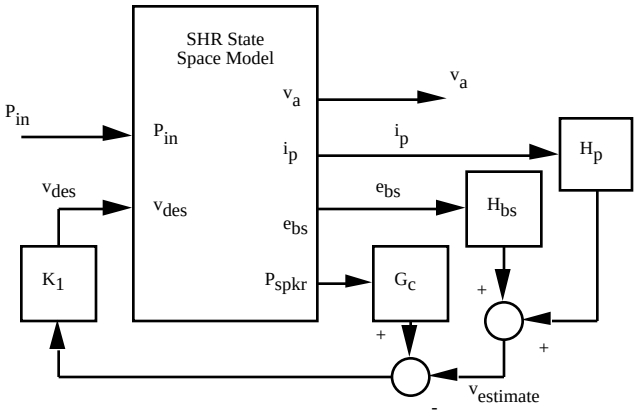

Figure 8: SHR Model Showing Closed-Loop HR Configuration

The frequency response of the closed-loop SHR system can be computed and compared to the ideal boundary condition for similar controller parameters. Figure 9 compares the two models for an integral controller with $K_P = K_D = 0$, and K_I ranging between 0 and 6.

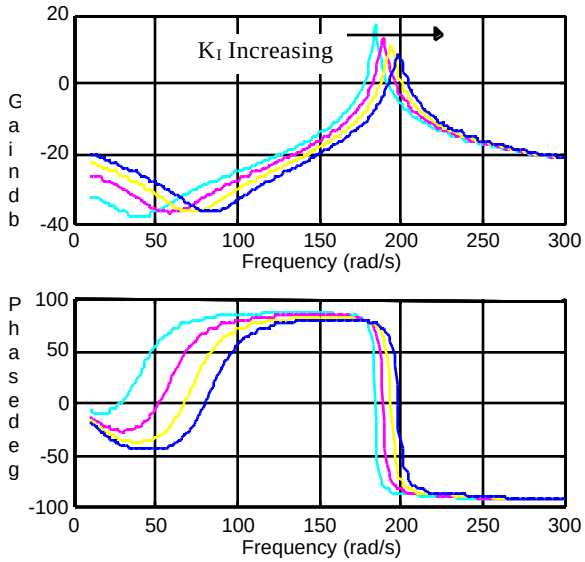

Figure 9: Bode Diagram of SHR for Integral Controller for K_I Ranging from 0 to 6.

These results show that while the introduction of the actuator into the model changes the dynamics somewhat, the desired resonance is preserved. Figure 9 clearly shows that varying K_I results in changing the system resonant frequency. This result indicates that the compensated acoustic actuator will perform the task of the complex boundary condition as hoped. Some differences between these results and the ideal boundary condition model response should be noted. In Figure 9 the peak value of the gain at resonance changes as K_I is modified in contrast to the ideal response given by (14), which shows that the gain become infinite at resonance since there is no damping in the model. Also, the low frequency response shown in Figure 9 differs from the ideal boundary condition model. This should be expected from the dynamics introduced into the system by the actuator. However, in all cases the resonance phenomenon is preserved and the effectiveness of the system as a acoustic vibration absorber is maintained.

CONCLUSIONS

The SHR system developed in this study represents a powerful new tool in tuning acoustic systems. The SHR adds a nominal resonance to any acoustic system and allows the resonance to be changed on-line, continuously over a range of frequencies. It has advantages over other technologies in that it does not add significant mechanical complexity, and the design places the sensitive sensor and actuator away from the direct path of the process. Future work in this area will include experimental model verification, and investigation of on-line control strategies.

REFERENCES

Birdsong, C., 1996, "*A compensated Actuator for an Acoustic Duct*", Masters Thesis, Michigan State University.

Garrett, K., 1992 , "*Inter-cylinder charge Robbing: Key factor in Induction-Tract Tuning*", Automotive Engineer v 17 n 4 Aug-Sep.

Grahm, C., Graves, M., Tenkel, R., 1992, "*General Motors High Performance 4.3L V6 Engine*", vol 101, sect 3, SAE transactions.

Jameson, R., Hodgins, P., 1990, "*Improvement of the Torque Characteristics of a Small, High-Speed Engine Through the Design of Helmholtz-Tuned Manifolding*", International Congress & Exposition, SAE, February.

Karnopp, D. C., 1990, Margolis, D.L. and Rosenberg, R.C., "*System Dynamics: A Unified Approach*", New York, John Wiley & Sons, Inc.

Kong, H. , Woods, R., 1992, "*Tuning of Intake Manifold of an Internal Combustion Engine Using Fluid Transmission Line Dynamics*", International Congress & Exposition, SAE, February.

Radcliffe C. J., Gogate, S. D., 1996, "*Velocity Feedback Compensation of Electromechanical Speakers for Acoustic Applications*", International Federation of Automatic Control, Triennial World Congress, July.

Radcliffe C.J., Gogate S.D., Hall G., 1994, "*Development of an Active Acoustic Sink (AAS) for Noise Control Applications*", Active Control of Vibrations and Noise, ASME.

Radcliffe, C. J., Gogate, S. D., 1992, "Identification and Modeling Speaker Dynamics for Acoustic Control Applications", ASME Symposium on Active Control of Noise and Vibration.

Temkin, 1936, "*Elements of Acoustics*", Wiley & Sons, Inc.